DEMONSTRATION OF GRADIENT ABOVE 300 MV/m IN SHORT PULSE REGIME USING AN X-BAND SINGLE-CELL STRUCTURE

J. Shao[1,*], X. Lin[2], M. Peng[1,2], H. Chen[2], S. Doran[1], G. Ha[1], C. Jing[1,†], W. Liu[1], J. Power[1],
J. Shi[2,‡], C. Whiteford[1], E. Wisniewski[1], H. Zha[2]

[1]Argonne National Laboratory, Lemont, IL, USA

[2]Tsinghua University, Beijing, China

Abstract

High gradient acceleration is one of the critical technologies required by future linear colliders, free-electron lasers, and compact linac-based applications. Among decade-long effort to break state-of-the-art gradient limitation of ~100 MV/m in normal conducting structures, using RF pulses shorter than 20 ns is a promising approach based on theoretic analysis and experimental observation. In this study, we demonstrated high gradient above 300 MV/m using an X-band 11.7 GHz single-cell travelling-wave structure with 6 ns FWHM RF pulses generated by a power extractor. In comparison, a scaled 11.424 GHz structure only reached below 150 MV/m driven by 30-100 ns RF pulses from a klystron with pulse compression. The experimental results and the suggested new mechanism of beam acceleration in the Breakdown Insensitive Acceleration Regime (BIAR) are presented in this manuscript.

INTRODUCTION

Gradient is a key figure of merit of linear accelerators to increase energy gain while maintaining facility footprint. Over the past decades, worldwide effort has been devoted to X-band normal-conducting accelerating structures driven by the challenging requirements of TeV-scale linear colliders. To date, ~120 MV/m and ~150 MV/m accelerating gradient have been respectively achieved in multi-cell and single-cell structures owing to continuous improvements of geometry optimization, high precision machining, high quality surface preparation, and understanding of RF breakdown. However, further breakthrough of gradient may rely on advanced acceleration concepts.

Acceleration using RF pulses shorter than 20 ns is a promising approach as predicted by the empirical scaling law of breakdown rate (BDR) [1] as well as proved in recent experiments by two-beam acceleration [2] and collinear wakefield acceleration [3]. In this study, we directly demonstrate the effectiveness of this approach where at least two-fold improvement of gradient has been obtained by shortening the RF pulses from 30-100 ns to 6 ns. Encouraged by the results, we propose the BIAR scheme in which the transmitted RF pulse and the accelerated beam remain intact even when RF breakdown occurs.

_____

* Now at Institute of Advanced Facilities, Shenzhen, China

† jingchg@anl.gov

‡ shij@tsinghua.edu.cn

STRUCTURE DESIGN

The X-band metallic disk-loaded single-cell travelling-wave accelerating structure (Fig. 1(a)) has been optimized for high transient gradient with 6 ns FWHM RF pulses (3 ns rising time, 3 ns flat-top, and 3 ns falling time) generated by power extractors available at Argonne Wakefiele Accelerator facility (AWA) [2, 4–6]. The transient gradient is defined as the one seen by an ultra-relativistic witness beam,

$$G(t_0) = \frac{\int_{l_1}^{l_2} E(z, t) dt}{l_2 - l_1}|_{t = t_0 + z/c} \qquad (1)$$

where E is the on-axis field, t_0 is the injection moment of the witness beam, and $l_{1,2}$ are the longitudinal boundaries.
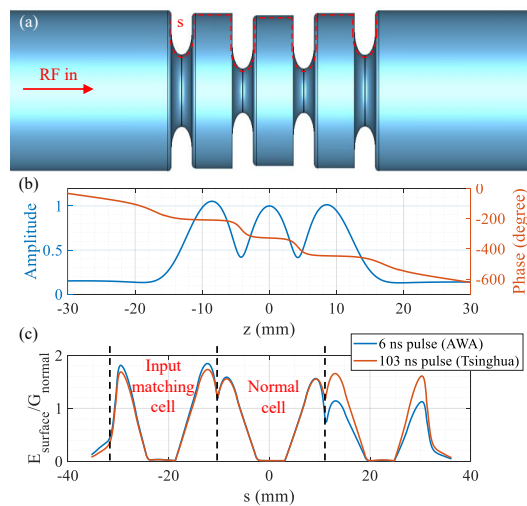

Figure 1: The X-band single-cell travelling-wave structure (a), the on-axis field (b), and the surface field along the contour (c).

The optimized structure consists of a normal cell and two matching cells designed by Kroll's method [7]. The resultant on-axis and surface field of the input matching cell are slightly higher than the normal one, therefore making it more vulnerable to RF breakdown, as illustrated in Fig. 1(b-c).

The simulated transient accelerating gradient is illustrated in Fig. 2. Using 6 ns FWHM RF pulses, the maximum transient accelerating gradient of the normal cell (denoted as $G_{normal,short}$) and the input matching cell (denoted as $G_{matching,short}$) reaches 80% and 92% of the theoretical steady value calculated from RF properties of the normal cell

MC7: Accelerator Technology

T06: Room Temperature RF

(denoted as G_{theory}) [8], respectively. Using long RF pulses with 20 ns rising and falling time at Tsinghua, the transient gradient of the normal cell and the input matching cell during the flat-top (denoted as $G_{normal,long}$ and $G_{matching,long}$) is 93% and 100% of G_{theory}, respectively. The small difference between $G_{normal,long}$ and G_{theory} is caused by the slight on-axis field distortion of the single normal cell introduced by the matching cells.
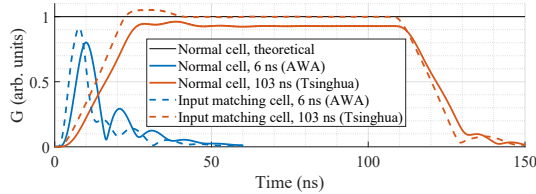

Figure 2: Transient gradient calculated by Eq. (1).

EXPERIMENTAL SETUP

The experimental setup at AWA is illustrated in Fig. 3. Drive beam with 8 bunches spaced at 769 ps was sent through a metallic disk-loaded power extractor [4], generating short RF pulses at the output coupler that fed into the accelerating structure and absorbed by the load. The input pulse and the transmitted pulse of the accelerating structures were monitored by directional couplers [4]. It should be noted that an elongated secondary input pulse could be observed ~25 ns after the main pulse, which was caused by double-reflection of the main pulse at the input coupler of the accelerating structure and the beam entrance of the power extractor.
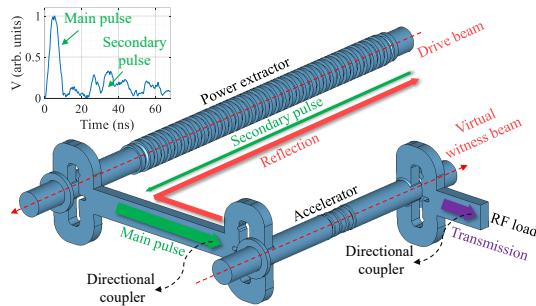

Figure 3: Experimental setup at AWA. Inset: typical input pulse shape to the accelerating structure.

The long pulse experiment at Tsinghua used a 50 MW X-band klystron with pulse compression [9] to drive the accelerating structure. Various pulse lengths from 30 ns to 100 ns could be obtained by adjust the LLRF system.

EXPERIMENTAL RESULTS

Short Pulse

The high-power test at AWA has accumulated ~ 7.7×10^4 pulses with 2 Hz repetition rate. We divide the entire test history (Fig. 4) into two regimes, the conditioning period when the input power (i.e. the drive beam charge) was continuously increased and the testing period after reaching the

maximum input power. Due to the relatively large drive beam charge fluctuation, we future divide all pulses according to $N_{normal,short}$ for following statistic analysis.
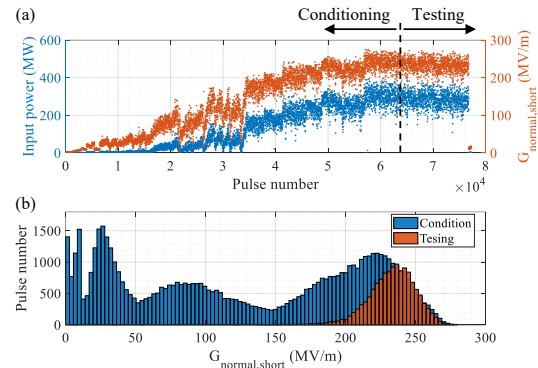

Figure 4: High-power test history at AWA (a) and the pulse distribution as a function of $N_{normal,short}$ (b).

Three typical pulse shapes could be identified from transmitted wave through the accelerating structure monitored at the RF load. In the normal condition (Fig. 5), the measured pulse shape, including the transmitted main and secondary pulses, agrees well with the predicted one convoluted by the input pulse shape and the measured S21 of the accelerating structure in cold test.
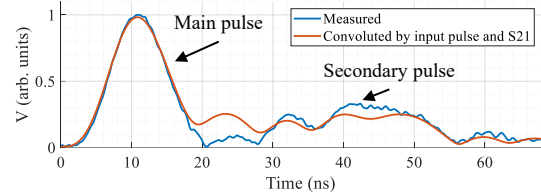

Figure 5: Normal transmitted pulse shape.

In the first abnormal case (Fig. 6), the measured main pulse distorts and the secondary one still transmits. The dependence of probability on gradient has two bands during conditioning and vanishes in testing. Therefore, we attribute this case as multipacting that could be caused by emission from initial surface defects [10].

In the second abnormal case (Fig. 7), the measured main pulse agrees with convolution while the secondary one is blocked. The probability exponentially depends on gradient and decreases after conditioning. Accordingly, we consider this case as RF breakdown.

Long Pulse

The high-power test at Tsinghua has accumulated ~ 2.3×10^7 pulses with up to 60 Hz repetition rate and the history is illustrated in Fig. 8.

Comparison

The dependence of BDR on gradient in both tests is illustrated in Fig. 9. The BDR of the short pulse experiment is relatively high due to the limited pulse number and it should

MC7: Accelerator Technology

T06: Room Temperature RF

13th Int. Particle Acc. Conf.
IPAC2022, Bangkok, Thailand
JACoW Publishing
ISBN: 978-3-95450-227-1
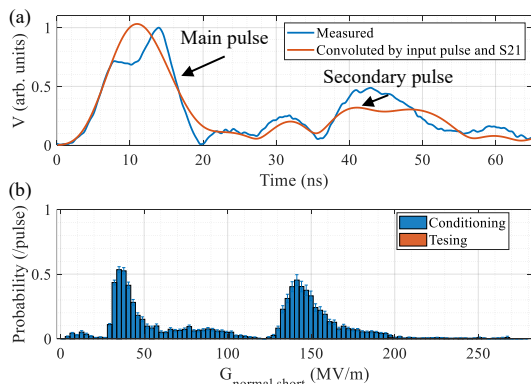ISSN: 2673-5490
doi:10.18429/JACoW-IPAC2022-FROXSP2

Figure 6: The first type of abnormal transmitted pulse shape (a) and its probability as a function of $N_{normal,short}$ (b).
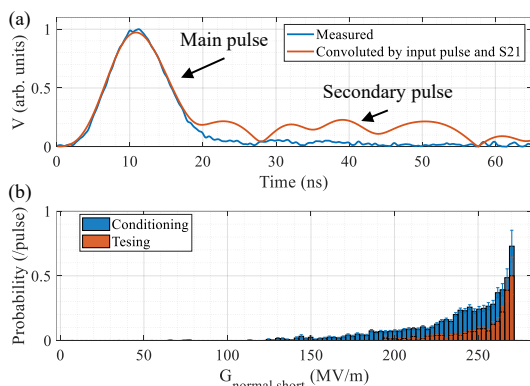

Figure 7: The second type of abnormal transmitted pulse shape (a) and its probability as a function of $N_{normal,short}$ (b).
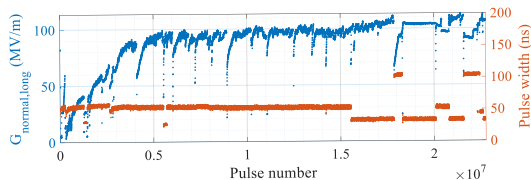

Figure 8: High-power test history at Tsinghua.

be able to be reduced by further conditioning. Therefore, we fit the long pulse data by $BDR \propto G^{30}$ [1] and extrapolate it for vivid comparison. At the same BDR, the short pulse gradients doubles the long pulse ones, with $G_{normal,short}$, $G_{matching,short}$, and the maximum surface field reaching 270 MV/m, 308 MV/m, and 500 MV/m, respectively.

DISCUSSION

In Fig. 9(a), the experimental results with 54 ns is further extrapolated to 6 ns by $BDR \propto \tau^5$ where τ is the pulse length [1]. The resultant gradient is still ~30 % lower than the short pulse experimental results at the same BDR and the deviation could be even larger considering the short pulse case in Fig. 9 only represents the detectable RF breakdown of the secondary pulse while the main pulse remains intact.
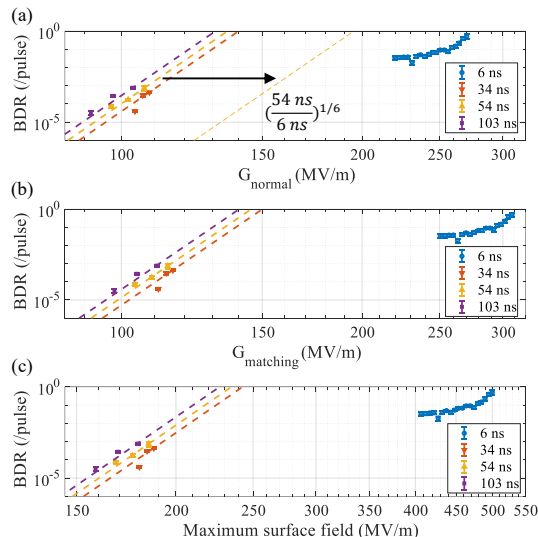

Figure 9: BDR as a function of (a) G_{normal}, (b) $G_{matching}$, and (c) maximum surface field. The thick dashed lines represent the exponential fitting results.

This observation indicates new breakdown mechanism in the short pulse regime.

We propose a hypothesis that RF breakdown triggered by the main pulse requires certain time to develop, i.e. the generated plasma from the iris surface with the highest field needs tens of ns to expand towards the iris and block RF transmission [11, 12]. In this case, the main pulse (shorter than 10 ns) can transmit through the structure normally but the following secondary pulse will be blocked by plasma. This mechanism encourages the Breakdown Insensitive Acceleration Regime where the RF pulse length is shorter than the RF breakdown development period so that RF transmission and beam acceleration won't be impacted by RF breakdown.

CONCLUSION

By comparing the performance of an X-band single-cell accelerating structure with various RF pulse lengths from 6-100 ns, we have directly demonstrated the effectiveness of using short pulse to improve gradient where accelerating gradient above 300 MV/m has been successfully obtained with no RF breakdown of the main pulse. We have studied the physics underlying the observation and proposed the BIAR concept that could benefit linac-base applications in general.

ACKNOWLEDGEMENT

REFERENCES

[1] A. Grudiev *et al.*, 'New local field quantity describing the high gradient limit of accelerating structures", *Phys. Rev. ST Accel. Beams*, vol. 12, p. 102001, 2009. `doi:10.1103/PhysRevSTAB.12.102001`

[2] C. Jing *et al.*, "Electron acceleration through two successive electron beam driven wakefield acceleration stages", *Nucl. Instrum. Methods Phys. Res. A*, vol. 898, no. 72, 2018. `doi:10.1016/j.nima.2018.05.007`

[3] M. Forno *et al.*, "rf breakdown tests of mm-wave metallic accelerating structures", *Phys. Rev. Accel. Beams*, vol. 19, p. 011301, 2016. `doi:10.1103/PhysRevAccelBeams.19.011301`

[4] J. H. Shao *et al.*, "Generation of High Power Short Rf Pulses using an X-Band Metallic Power Extractor Driven by High Charge Multi-Bunch Train", in *Proc. IPAC'19*, Melbourne, Australia, May 2019, pp. 734–737. `doi:10.18429/JACoW-IPAC2019-MOPRB069`

[5] J. Shao *et al.*, "Development and high-power testing of an X-band dielectric-loaded power extractor", *Phys. Rev. Accel. Beams*, vol. 23, p. 011301, 2020. `doi:10.1103/PhysRevAccelBeams.23.011301`

[6] J. Picard *et al.*, "Generation of 565 MW of *X*-band power using a metamaterial power extractor for structure-based wakefield acceleration", *Phys. Rev. Accel. Beams*, vol. 25, p.051301, 2022. `doi:10.1103/PhysRevAccelBeams.25.051301`

[7] N. M. Kroll, D. C. Vier, and C. K. Ng, "Applications of Time Domain Simulation to Coupler Design for Periodic Structures", in *Proc. LINAC'00*, Monterey, CA, USA, Aug. 2000, paper TUE04, pp. 614–617.

[8] M. M. Peng *et al.*, "Optimization of a Single-Cell Accelerating Structure for Rf Breakdown Test With Short Rf Pulses", in *Proc. NAPAC'19*, Lansing, MI, USA, Sep. 2019, paper WEPLM67, pp. 747–750.

[9] Y. Jiang *et al.*, "A Compact X-Band Microwave Pulse Compressor Using a Corrugated Cylindrical Cavity", *IEEE Trans. Microw. Theory Tech.*, vol. 69, pp. 1586-1593, 2021. `doi:10.1109/TMTT.2021.3053913`

[10] H. Xu *et al.*, "Measurement of internal dark current in a 17 GHz, high gradient accelerator structure", *Phys. Rev. Accel. Beams*, vol. 22, p. 021002, 2019. `doi:10.1103/PhysRevAccelBeams.22.021002`

[11] F. Wang and C. Adolphsen, "Localization of rf breakdowns in a standing wave cavity", *Phys. Rev. ST Accel. Beams*, vol. 12, p. 042001, 2009. `doi:10.1103/PhysRevSTAB.12.042001`

[12] J. Shao *et al.*, "Observation of temporal evolution following laser triggered rf breakdown in vacuum", *Phys. Rev. ST Accel. Beams*, vol. 17, p. 072002, 2014. `doi:10.1103/PhysRevSTAB.17.072002`